action in Figure 5 began with only copper(II) tetraglycine. An initiation reaction is required in order to produce the initial 5×10^{-9} M $Cu^{III}(H_{-3}G_4)^-$ found from the intercept of the log plot in Figure 5. The initiation reaction proposed for the autocatalytic autoxidation of copper(II) tetraglycine is the disproportionation of $Cu^{II}(H_{-2}G_4)^-$ as in eq 40. The equilibrium constant was estimated to be 10^{-8} (μ = 1.0 M(NaClO$_4$)).[5] From the conditions used for the reaction illustrated in Figure 5, the equilibrium constant for the reaction in eq 40 predicts 1.4×10^{-8} M $Cu^{III}(H_{-3}G_4)^-$ initially, certainly a reasonable initiation step. The reaction of sulfite and oxygen, eq 41, is also a reasonable initiation step. The SO_5^{2-} produced

$$2Cu^{II}(H_{-2}G_4)^- \rightleftarrows Cu^{I}(H_{-1}G_4)^- + Cu^{III}(H_{-3}G_4)^- \quad (40)$$

$$SO_3^{2-} + O_2 \rightarrow SO_5^{2-} \quad (41)$$

can then generate the initial $Cu^{III}(H_{-3}G_4)^-$ by oxidizing the $Cu^{II}(H_{-3}G_4)^{2-}$ reactant. The mechanism by which the reaction in eq 41 occurs is not entirely clear. The possibility of a multistep process in which trace-metal catalysis takes part has not been ruled out; however, this type of catalysis must be considerably slower than the copper peptide catalysis.

Conclusions

The anaerobic reduction of $Cu^{III}(H_{-3}G_4)^-$ by sulfite proceeds stoichiometrically via two reversible one-electron-transfer steps. Kinetic evidence strongly supports the sulfite radical anion as a product of the first electron transfer. An upper limit for the formal potential of the sulfite radical anion has been estimated from kinetic considerations to be +0.89 V. Hydrogen sulfite was found to be 30 times slower as a reductant than sulfite.

Oxygen, in the presence of added $Cu^{II}(H_{-3}G_4)^{2-}$, prompts a sulfite-induced oxidation to form $Cu^{III}(H_{-3}G_4)^-$. The $Cu^{III}(H_{-3}G_4)^-$ autocatalytically accelerates the induced oxidation reaction. The switching redox nature of the sulfite–O_2 reaction and the observed oscillations in the concentration of $Cu^{III}(H_{-3}G_4)^-$ are regulated by the relative rates at which $Cu^{III}(H_{-3}G_4)^-$ and oxygen compete for the sulfite radical. Facile electron transfer makes the copper peptide complex a catalyst for the autoxidation of sulfite. The efficiency of the catalysis

$$SO_3^{2-} + {}^1/_2O_2 \xrightarrow{Cu(II/III)} SO_4^{2-} \quad (42)$$

is limited, however, by the rate at which sulfur-based oxidizing intermediates are lost by pathways other than those leading to the autocatalytic formation of $Cu^{III}(H_{-3}G_4)^-$.

Acknowledgment. This investigation was supported by Public Health Service Grant No. GM 19775 from the National Institute of General Medical Sciences.

Registry No. $Cu^{III}(H_{-3}G_4)^-$, 57692-61-2; SO_3^{2-}, 14265-45-3; HSO_3^-, 15181-46-1; $Cu^{II}(H_{-3}G_4)^{2-}$, 57603-18-6; O_2, 7782-44-7.

Contribution from the Department of Chemistry,
East Texas State University, Commerce, Texas 75428

Kinetic and Equilibrium Study of the Reaction of (*meso*-Tetrakis(*p*-sulfonatophenyl)porphyrinato)diaquocobaltate(III) with Pyridine in Aqueous Solution

KENNETH R. ASHLEY* and JOHAN G. LEIPOLDT[1]

Received August 26, 1980

The reaction of pyridine (py) with (*meso*-tetrakis(*p*-sulfonatophenyl)porphyrinato)diaquocobaltate(III) ($Co(TPPS)(H_2O)_2^{3-}$) has been investigated between pH 2 and 13 at μ = 1.00 M (NaClO$_4$). Scheme I best depicts the reactions deduced to be important. The values of all of the parameters in Scheme I were determined and are reported. The k_1^{py} path is second order with $k_1^{py} = (9.56 \pm 0.30) \times 10^2$ M^{-1} s^{-1} at 25 °C and the values of the activation parameters are $\Delta H^*_1 = 17.6 \pm 0.4$ kcal/mol and $\Delta S^*_1 = 14.4 \pm 1.3$ cal/(deg mol). These parameters imply dissociative (d) activation. The k_4^{py} path is second order with $k_4^{py} = (1.22 \pm 0.12) \times 10^6$ M^{-1} s^{-1} at 25 °C, and the values of the activation parameters are $\Delta H^*_4 = 11.5 \pm 0.5$ kcal/mol and $\Delta S^*_4 = 6.4 \pm 1.6$ cal/(deg mol). The parameters imply d activation and the OH$^-$ ligand has labilized the $Co(TPPS)(OH)H_2O^{4-}$ by a factor of 10^3 compared to $Co(TPPS)(H_2O)_2^{3-}$. The k_2^{py} path has a pseudo-first-order rate law with the pseudo-first-order rate constant $k_{obsd} = (E[py] + FG)/(G + [pyl])$ at pH 13. This is interpreted to imply a dissociative (D) mechanism. The parameter E represents the first-order rate constant for formation of the 5-coordinate intermediate and has a value of $(1.57 \pm 0.13) \times 10^3$ s^{-1} at 25 °C. The values of ΔH^*_7 and ΔS^*_7 are 11.6 ± 3.1 kcal/mol and -5.1 ± 10.1 cal/(deg mol). The values of K_{a1}, K_{a2}, and K_{a1}^{py} at 25 °C are $(9.4 \pm 0.6) \times 10^{-8}$, $(1.7 \pm 0.2) \times 10^{-10}$, and $(5.6 \pm 0.2) \times 10^{-10}$ M, respectively. The values of K_1^{py}, K_2^{py}, K_4^{py}, K_5^{py}, and K_6^{py} at 25 °C are $(9.1 \pm 0.9) \times 10^8$ M^{-1}, $(1.2 \pm 0.1) \times 10^5$ M^{-1}, $(5.4 \pm 0.8) \times 10^6$ M^{-1}, $(1.3 \pm 0.2) \times 10^2$, and 3.4 ± 0.7, respectively. In summary, the kinetic and equilibrium properties of $Co(TPPS)(H_2O)_2^{3-}$ are very similar to those of (*meso*-tetrakis(4-*N*-methylpyridyl)porphyrin)diaquocobalt(III) and (*meso*-tetrakis(4-carboxyphenyl)porphyrinato)diaquocobaltate(III). However there are some significant differences.

Introduction

The substitution reactions of cobalt(III) porphyrins have been of continuing interest.[2-10] The most striking thing about these reactions is the unusual lability of the compounds. The anation reactions were concluded to occur by a D or an I$_d$ mechanism. Ashley and Au-Young have reported the results of the anation reactions of NCS$^-$, I$^-$, Br$^-$, and Cl$^-$ with (*meso*-tetrakis(*p*-sulfonatophenyl)porphyrinato)diaquocobaltate(III), ($Co(TPPS)(H_2O)_2^{3-}$).[9] This paper reports the results of the investigation of the reaction of C_5H_5N(py), between pH 2 and 13.0 with $Co(TPPS)(H_2O)_2^{3-}$.

---

(1) On leave of absence from the Chemistry Department, University of the Orange Free State, Bloemfontein, Republic of South Africa.
(2) Fleischer, E. B.; Jacobs, S.; Mestichelli, L. *J. Am. Chem. Soc.* **1968**, *90*, 2527.
(3) Pasternack, R. F.; Cobb, M. A. *Biochem. Biophys. Res. Commun.* **1973**, *51*, 507.
(4) Pasternack, R. F.; Cobb, M. A. *J. Inorg. Nucl. Chem.* **1973**, *35*, 4327.
(5) Fleischer, E. B.; Krishnamuthy, M. *Ann. N.Y. Acad. Sci.* **1973**, *206*, 32.
(6) Ashley, K. R.; Berggren, M.; Cheng, M. *J. Am. Chem. Soc.* **1975**, *97*, 1422.
(7) Pasternack, R. F.; Cobb, M. A.; Sutin, M. *Inorg. Chem.* **1975**, *14*, 866.
(8) Ashley, K. R. *J. Inorg. Nucl. Chem.* **1976**, *39*, 357.
(9) Ashley, K. R.; Au-Young, S. *Inorg. Chem.* **1976**, *15*, 1937.
(10) Pasternack, R. F.; Parr, G. R. *Inorg. Chem.* **1976**, *15*, 3087.

0020-1669/81/1320-2326$01.25/0 © 1981 American Chemical Society

Scheme I

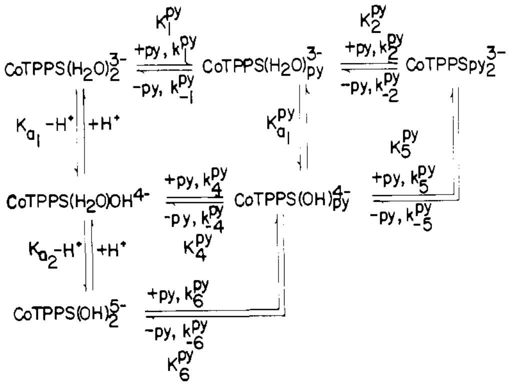

Table I. Molar Absorptivities of the Compounds Studied [μ = 1.00 M (NaClO$_4$)]

compd	λ_{max}, nm	$10^{-5}\epsilon_{max}$, M^{-1} cm^{-1}
Co(TPPS)(H_2O)$_2^{3-}$	425	2.38
Co(TPPS)(H_2O)(OH)$^{4-}$	426	2.18
Co(TPPS)(OH)$_2^{5-}$	429	1.85
Co(TPPS)(H_2O)(py)$^{3-}$	425.5	2.23
Co(TPPS)(OH)(py)$^{4-}$	426	2.13
Co(TPPS)(py)$_2^{3-}$	433	1.83

Experimental Section

Materials. Sodium *meso*-tetrakis(*p*-sulfonatophenyl)porphyrin (Na_4TPPS) was obtained from Man-Win Co. of Washington, D.C. The cobalt was inserted, and the $Na_3[Co(TPPS)(OH_2)_2]$ was purified in the following manner. Approximately 50 mg of Na_4TPPS and 140 mg of $CoSO_4 \cdot 7H_2O$ (1:10 mole ratio) were added to 25 mL of 0.7 M aqueous acetic acid. The solution was heated on a steam bath for 30 min while oxygen was bubbled through it. The solution then was passed through a 1 × 30 cm acid washed alumina column. The alumina had been dried at 120 °C overnight. The column was eluted with 0.01 M NaOH. The effluent that was pH 9 or below was collected. The effluent that was above pH 9 was collected separately and passed through another alumina column as before. The combined effluents that were below pH 9 were evaporated on a steam bath to 10 mL. This solution was passed through a Sephadex G-10 column to separate the light molecular weight impurities. The effluent was dried on a steam bath and then dried overnight at 120 °C. The elemental analysis was performed by Galbraith Laboratories, Inc., and the cobalt analysis was performed in this laboratory with use of a Perkin-Elmer 303 atomic adsorption instrument. Anal. Calcd. for $Na_3Co(TPPS)(H_2O)_2$, $Na_3CoC_{44}H_{28}N_4S_4O_{14}$: C, 48.38; H, 2.56; N, 5.13; S, 11.72; Co, 5.39; Found: C, 45.48; H, 3.59; N, 5.78; S, 10.52; Co, 5.39.

Equilibrium and Kinetic Measurements. The equilibrium and kinetic measurements were made essentially as reported previously.[6,9] No buffers were used except for a 0.01 M sodium borate buffer between pH 8.2 and 9.8. Blank experiments confirmed that no reaction occurred between the buffer and the Co(TPPS)(H_2O)$_2^{3-}$. The ionic strength was maintained constant at 1.00 M (NaClO$_4$).

Results

Scheme I defines the system under investigation. The rate constant for a reaction will be used to label that path. Although all reaction paths have been delineated, they are not all applicable in this study. The molar absorptivities of the Soret band of the compounds of interest are reported in Table I.

Acid Dissociation Constants. A plot of A_{424} vs. pH (Figure 1) clearly showed that the Co(TPPS)(H_2O)$_2^{3-}$ is diprotic. It was obvious that the two steps were separated enough so that the evaluation of K_{a_1} and K_{a_2} could be performed separately. From the equilibrium constant expression, the mass balance, and Beer's law, eq 1 could be derived. A_a was the absorbance

$$A = (K_{a_i}A_b + A_a[H^+])/(K_{a_i} + [H^+]) \qquad (1)$$

at 424 nm of the acid form and A_b was the absorbance at 424 nm of the base form. The data was fit to eq 1 with use of a nonlinear least-squares program.[11] This program was used in all of the curve fittings, and all of the reported uncertainties are one standard deviation. The calculated values of A_a and A_b agreed within experimental error with the measured values. The values of K_{a_1} and K_{a_2} are in Table II. The values of $\Delta H°_{a_i}$ and $\Delta S°_{a_i}$ were determined with the use of eq 2. The values

$$K_{a_i} = e^{\Delta S°_{a_i}/R}e^{-\Delta H°_{a_i}/RT} \qquad (2)$$

of K_{a_i} were weighed as $1/\sigma_{a_i}^2$, where $\sigma_{a_i}^2$ was the variance of each K_{a_i} at each temperature. The values of ΔH° and ΔS° are −6.43 ± 1.01 kcal/mol and −53.8 ± 3.5 cal/(deg mol) and 8.23 ± 0.99 kcal/mol and −17.3 ± 1.5 cal/(deg mol), respectively, for K_{a_1} and K_{a_2}. The calculated values of K_{a_1} and K_{a_2} at 45 °C were (4.6 ± 10.8) × 10^{-8} and (3.7 ± 5.4) × 10^{-10} M, respectively. The uncertainties are the estimated standard deviations derived from the uncertainties in $\Delta H°_{a_i}$ and $\Delta S°_{a_i}$.

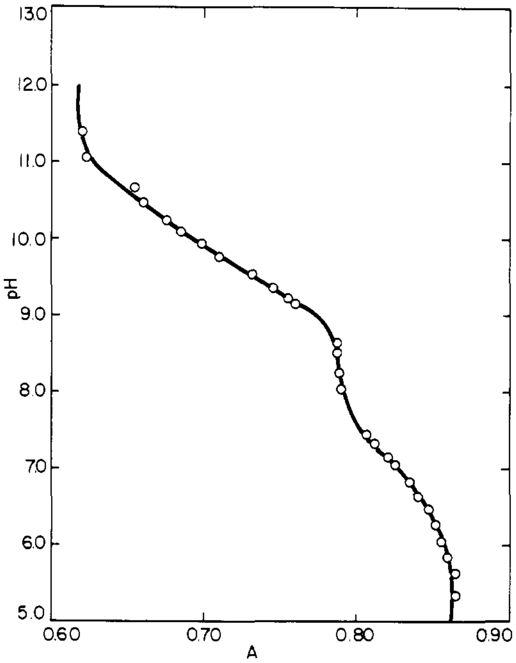

Figure 1. Plot of *A* vs. pH at 25 °C, λ = 424 nm, and μ = 1.00 M (NaClO$_4$) for the determination of K_{a_1} and K_{a_2}. The solid line is the computer fit of the data to eq 1.

Table II. Acid Dissociation Constants of the Compounds in Scheme I

temp, °C	$10^7K_{a_1}$, M	$10^{10}K_{a_2}$, M	$10^9K_{a_1}^{py}$, M
15	0.131 ± 0.025	0.936 ± 0.57	
25	0.937 ± 0.063	1.72 ± 0.16	0.563 ± 0.019
35	5.65 ± 1.15	2.36 ± 0.18	0.776 ± 0.069
45			1.28 ± 0.04

Stability Constants. The values of K_2^{py}, K_5^{py}, and K_6^{py} were determined spectrophotometrically. The absorbance was measured as the ligand concentration was varied. From Beer's law, the mass balance, and the stability constant expression for K_2^{py}, eq 3 can be derived. *A* is the absorbance of a solution

$$A = (A_r + A_pK_2^{py}[py])/(1 + K_2^{py}[py]) \qquad (3)$$

of the cobalt porphyrin and py, A_r is the absorbance of a solution of the reactant, and A_p is the absorbance of the

---

[11] Moore, R. H. Report LA 2367; Los Alamos Scientific Laboratory: Los Alamos, NM, March 1960, and addend, January 1963 (modified by N. Roberts of East Texas State University for an IBM 360/50).

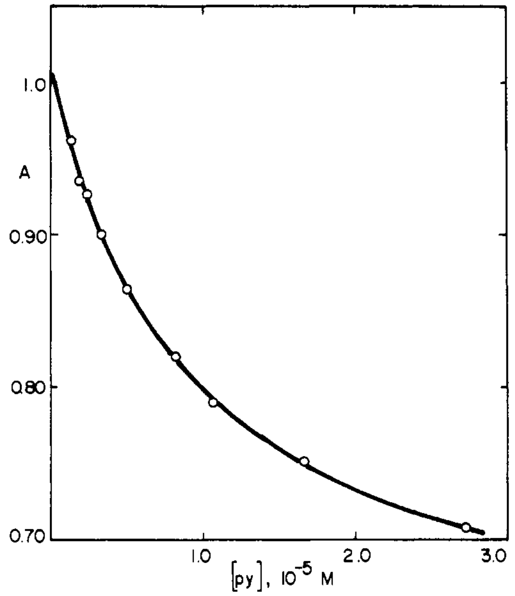

Figure 2. Plot of A vs. [py] at 25 °C, $\lambda = 433$ nm, and $\mu = 1.00$ M ($NaClO_4$) for the determination of K_2^{py}. The solid line is the computer fit of the data to eq 3.

Table III. Stability Constants at 25 °C for the Compounds in Scheme 1

parameter	value, M^{-1}
$K_1^{py}(k_1^{py}/k_{-1}^{py})$	$(3.13 \pm 0.62) \times 10^5$
$K_1^{py}(K_{a_1}k_4^{py}/K_{a_1}^{py}k_{-4}^{py})$	$(9.05 \pm 0.90) \times 10^8$
$K_1^{py}(K_{a_1}K_{a_2}K_6^{py}/K_{a_1}^{py}K_w)$	$(2.26 \pm 0.05) \times 10^8$
$K_2^{py}(k_2^{py}/k_{-2}^{py})$	$(8.38 \pm 1.29) \times 10^4$
$K_2^{py}(K_{a_1}^{py}K_5^{py}/K_w)$	$(1.19 \pm 0.26) \times 10^5$
K_2^{py}	$(1.15 \pm 0.09) \times 10^5$
$K_4^{py}(K_{a_2}K_6^{py}/K_w)$	$(1.36 \pm 0.28) \times 10^6$
$K_4^{py}(k_4^{py}/k_{-4}^{py})$	$(5.44 \pm 0.80) \times 10^6$
K_5^{py}	$(1.28 \pm 0.23) \times 10^2$
K_6^{py}	3.41 ± 0.65

product. The solid line in Figure 2 is the fit of the data to eq 3.

In the case of K_5^{py} and K_6^{py}, the values of the stability constants were close enough so that an equation such as eq 3 could not be used. From Beer's law and the mass balance and the stability constant expressions, eq 4 could be derived.

$$A = \frac{A_0 + A_1K_6^{py\prime}[py] + A_2K_6^{py\prime}K_5^{py\prime}[py]^2}{1 + K_6^{py\prime}[py] + K_6^{py\prime}K_5^{py\prime}[py]^2} \quad (4)$$

A is the absorbance of a solution of the cobalt porphyrin and py, A_0 is the absorbance of the solution of $Co(TPPS)(OH)_2^{5-}$, A_1 is the absorbance of the solution of $Co(TPPS)(py)OH^{4-}$, A_2 is the absorbance of the solution of $Co(TPPS)(py)_2^{3-}$, $K_5^{py\prime} = K_5^{py}/[OH^-]$, and $K_6^{py\prime} = K_6^{py}/[OH^-]$. The value of $[OH^-]$ was 0.100 M. The solid line in Figure 3 is the least-squares fit of the data to eq 4. Tabulated in Table III are the values of the stability constants. K_1^{py} and K_4^{py} were too large to determine spectrophotometrically. In Table III are reported also the values of stability constants calculated from other constants. The values of K_w at $\mu = 1.00$ M is $(1.62 \pm 0.08) \times 10^{-14}$ at 25 °C.[12] The values of K_w at 35 and 45 °C were calculated from the reported values of $\Delta H°$ and $\Delta S°$ at $\mu = 0.5$ M.[12]

Kinetics. The reaction of py with $Co(TPPS)(H_2O)_2^{3-}$ was studied at pH 2, various temperatures, and various py concentration. The total py concentration did not exceed 0.3 M and $\mu = 1.00$ M ($NaClO_4$). The free py concentration was calculated from the known total py concentration, the measured pH, and the reported value of 4.07×10^{-6} M for K_a at 25 °C.[13] The assumption was made that $[H^+] = 10^{-pH}$. The values of K_a for py at 35 and 45 °C were calculated to be 5.25×10^{-6} and 6.92×10^{-6} M from reported $\Delta H°$ value at $\mu = 0.5$.[13] The $Co(TPPS)(H_2O)_2^{3-}$ concentration was about 3.4×10^{-6} M at 25.0, 37.0, and 45.0 °C. The reaction, as well as all studied in this investigation, followed pseudo-first-order kinetics with

$$k_{obsd} = a + b[py] \quad (5)$$

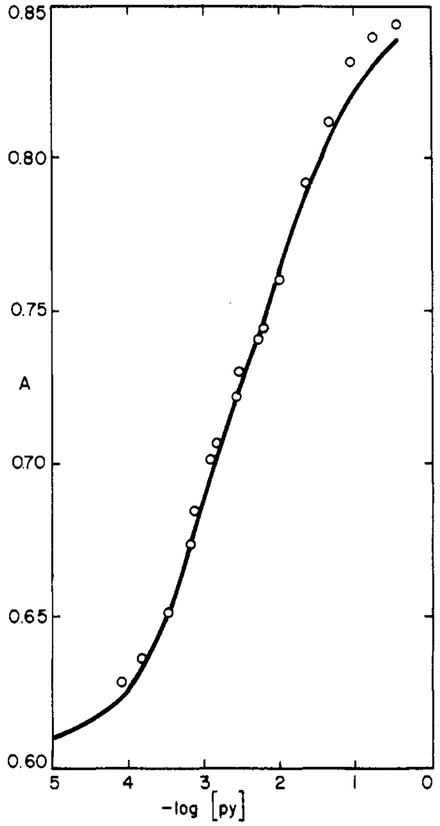

Figure 3. Plot of A vs. -log [py] at 25 °C, $\lambda = 433$ nm, $[OH^-] = 0.100$, and $\mu = 1.00$ M ($NaClO_4$) for the determination of K_5^{py} and K_6^{py}. The solid line is the computer fit of the data to eq 4.

The constants a and b were interpreted to be k_{-1}^{py} and k_1^{py}, respectively (Scheme I). The results are reported in Figure 4 and Table IV. The activation parameters were calculated with the use of the Eyring–Polanyi equation and are reported in Table IV.[14]

As the pH is increased from pH 2, the k_4^{py} and/or K_6^{py} path becomes increasingly important. Under the pseudo-first-order conditions employed in this investigation, the formation of $Co(TPPS)(py)_2^{3-}$ occurred also (path k_2^{py}); vide infra. This gave rise to biphasic kinetics of which the interpretation became ambiguous because of the difficulty of assigning the fast and slow steps to what reaction. Under the conditions of higher pH, but below pH 12, at which $Co(TPPS)_4(py)_2^{3-}$ does not form, the reaction is too fast to measure by stopped-flow techniques. Hence, the k_4^{py} and/or k_6^{py} reaction was studied above pH 12.

Figure 5 shows the plot of k_{obsd} vs. $[OH^-]$ at 1.02×10^{-3} M py, and Figure 6 shows the plot of k_{obsd} vs. [py] at 0.100

---

(12) Smith, R. M.; Martell, A.E. "Critical Stability Constants"; Plenum Press: New York, 1975; Vol. 4, p 1.

(13) Smith, R. M.; Martell, A. E. "Critical Stability Constants"; Plenum Press: New York, 1975; Vol. 2 p 165.

(14) Laidler, J. "Chemical Kinetics", 2nd ed.; McGraw-Hill: New York, 1965.

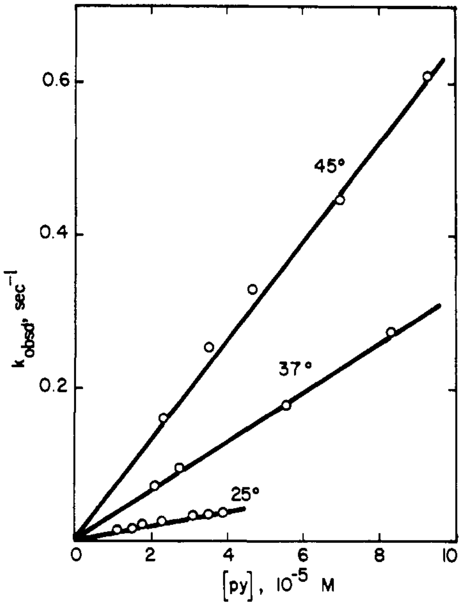

Figure 4. Dependence of k_{obsd} upon [py] for the k_1^{py} path at pH 2.00 and μ = 1.00 M ($NaClO_4$). The solid lines are the computer fit of the data to eq 5.

Table IV. Rate Constants and Activation Parameters for Schemes 1 and 11

temp, °C	$10^{-3}k_1^{py}$, M^{-1} s^{-1} [a]	$10^3k_{-1}^{py}$, s^{-1} [a]
25	0.956 ± 0.03	3.04 ± 0.59
37	3.24 ± 0.11	4.32 ± 3.3
45	6.53 ± 0.33	14.7 ± 12.8
ΔH^*_1 = 17.6 ± 0.4 kcal/mol, ΔS^*_1 = 14.4 ± 1.3 cal/(deg mol)		
temp, °C	$10^{-3}k_2^{py}$, M^{-1} s^{-1} [a]	$10^2k_{-2}^{py}$, s^{-1} [a]
25	3.16 ± 0.13	3.77 ± 0.56
35	7.07 ± 0.44	4.62 ± 2.37
45	12.5 ± 0.2	16.6 ± 1.6
ΔH^*_2 = 12.1 ± 0.5 kcal/mol, ΔS^*_2 = −1.82 ± 1.45 cal/(deg mol)		
temp, °C	$10^{-6}k_4^{py}$, M^{-1} s^{-1}	k_{-4}^{py}
25	1.22 ± 0.12[b]	0.245 ± 0.021[b]
25	1.31 ± 0.15[c]	0.241 ± 0.022[c]
35	2.59 ± 0.34[c]	0.659 ± 0.066[c]
45	4.49 ± 1.05[c]	1.45 ± 0.24[c]
ΔH^*_4 = 11.5 ± 0.5 kcal/mol, ΔS^*_4 = 6.4 ± 1.6 cal/(deg mol)		
temp, °C	$10^{-3}k_7$, s^{-1}	k_8/k_9, M
25	1.57 ± 0.13	0.444 ± 0.037
35	2.40 ± 0.35	0.451 ± 0.074
45	5.8 ± 0.66	0.517 ± 0.077
ΔH^*_7 = 11.6 ± 3.1 kcal/mol, ΔS^*_7 = −5.1 ± 10.1 cal/(deg mol)		

[a] pH 2.0. [b] $[OH^-]$ = 0.100 M. [c] [py] = 1.02 × 10^{-3} M.

M OH^- at 25 °C, where k_{obsd} is the pseudo-first-order rate constant. It is clear that the reaction is first order in py. Also the nonzero intercept in Figure 6 implies a path py independent or, more likely, a reverse reacton. The shape of the k_{obsd} vs. $[OH^-]$ plot indicates an inverse $[OH^-]$ dependence.

A cursory examination of the values of k_1^{py} and the concentration of $Co(TPPS)(H_2O)_2^{3-}$ at these conditions revealed that the k_1^{py} reaction path is unimportant. Assuming that only the k_4^{py} and k_6^{py} paths were important, eq 6 could be derived.

$$k_{obsd} = \frac{k_4^{py}K_w[py] + k_6^{py}K_{a_2}[py][OH^-]}{K_{a_2}[OH^-] + K_w} + k_{-4}^{py} + k_{-6}^{py}[OH^-] \quad (6)$$

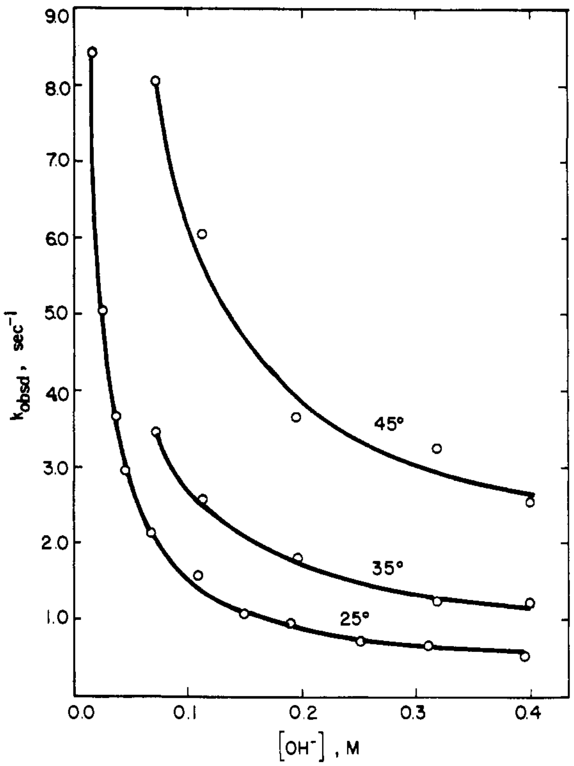

Figure 5. Dependence of k_{obsd} upon $[OH^-]$ at [py] = 1.02 × 10^{-3} M and μ = 1.00 M ($NaClO_4$). The solid lines are the computer fit of the data to eq 7 (see text).

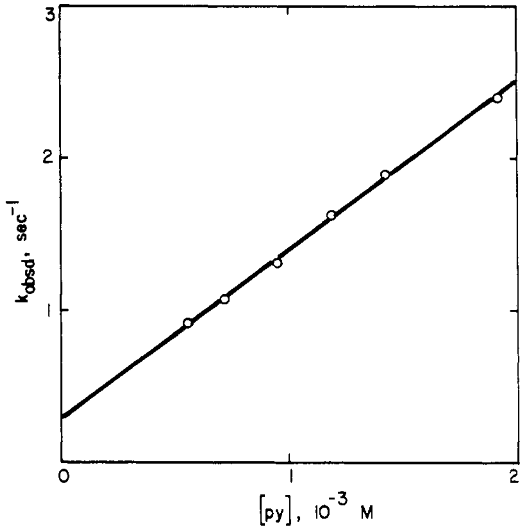

Figure 6. Dependence of k_{obsd} upon [py] at $[OH^-]$ = 0.100, μ = 1.00 M ($NaClO_4$) and 25 °C. The solid line is the computer fit of the data to eq 8 (see text).

At the $[OH^-]$ concentrations in these studies, $K_{a_2}[OH^-] \gg K_w$ and eq 7 resulted. A plot of k_{obsd} vs. $1/[OH^-]$ gave a very good

$$k_{obsd} = \frac{k_4^{py}K_w[py]}{K_{a_2}[OH^-]} + (k_6^{py}[py] + k_{-4}^{py} + k_{-6}^{py}[OH^-]) \quad (7)$$

straight line. This implied that the k_{-6}^{py} path was negligible under these condition. The solid lines in Figure 5 are the computer fit of the data to eq 7 with the $k_{-6}^{py}[OH^-]$ term deleted, i.e., $k_{obsd} = (A/[OH^-]) + B$. The value of A was 0.126 ± 0.003 M^{-1} s^{-1}, and the value of B was 0.241 ± 0.022 s^{-1} at 25 °C.

If [py] was varied while $[OH^-]$ was kept constant, eq 8 resulted. The solid line in Figure 6 is the computer fit of the

$$k_{\text{obsd}} = \left(\frac{k_4^{\text{py}} K_{\text{w}}}{K_{\text{a}_2}[\text{OH}^-]} + k_6^{\text{py}} \right) [\text{py}] + k_{-4}^{\text{py}} \quad (8)$$

data at 25 °C, i.e., $k_{\text{obsd}} = C[\text{py}] + D$. The value of C was $(1.12 \pm 0.02) \times 10^3$ M^{-1} s^{-1}, and the value of D was 0.283 ± 0.023 s^{-1}.

These results give $B = k_6^{\text{py}}[\text{py}] + k_{-4}^{\text{py}} = 0.241 \pm 0.022$ s^{-1} and $D = k_{-4}^{\text{py}} = 0.283 \pm 0.020$ s^{-1}. Since these two numbers are very similar and since the value of B was smaller than the value of D, it was concluded that $k_6^{\text{py}}[\text{py}]$ was negligible.

The value of k_4^{py} derived from A ($k_4^{\text{py}} K_{\text{w}}[\text{py}]/K_{\text{a}_2}$) was $(1.31 \pm 0.15) \times 10^6$ M^{-1} s^{-1}. The value of k_4^{py} derived from C $((k_4^{\text{py}} K_{\text{w}}/K_{\text{a}_2}[\text{OH}^-]) + k_6^{\text{py}})$, with the assumption that k_6^{py} was negligible, was $(1.22 \pm 0.12) \times 10^6$ M^{-1} s^{-1}. Since these two calculated values of k_4^{py} are the same, the assumption that k_6^{py} was negligible is correct. Similar results were obtained at 35 and 45 °C. The values of k_4^{py} and k_{-4}^{py} and the activation parameters are reported in Table IV.

The addition of the second py also was studied over a wide pH range. At pH 2 and the lowest free py concentration, over 55% of the complex was in the form $\text{Co(TPPS)}_4(\text{py})_2^{3-}$ at the end of the reaction. This second step (k_2^{py}) was not observed kineticly because it was faster than the first step. The second step was studied by adding 0.03 M total py to the $\text{Co(TPPS)(H}_2\text{O)}_2^{3-}$ solution at pH 2 before mixing. This ensured that all of the complex was in the form $\text{Co(TPPS)}_4(\text{H}_2\text{O})\text{py}^{3-}$ or $\text{Co(TPPS)}_4(\text{py})_2^{3-}$ (>50%). When additional py was added, only the second step was observed. The rate law for this step was pseudo first order in $[\text{Co(TPPS)(H}_2\text{O)}_2^{3-}]_{\text{total}}$ with the pseudo-first-order rate constant having the form of eq 5 (Figure 7). The values of a and b were assigned to k_{-2}^{py} and k_2^{py}, respectively. These values at the various temperatures are reported in Table IV along with the activation parameters. It will be seen below that eq 5 is a special form of a more general expression for k_{obsd} for the k_2^{py} path that develops at higher py concentration.

The addition of the second py at various temperatures was studied between pH 8.47 to 9.72 at [py] = 5.11×10^{-5} M. The k_4^{py} path was too fast to be observed kineticly in this pH region. The results are in Figure 8. From Scheme I, k_{obsd} could be defined by eq 9. However, a least-squares fit of the data to

$$k_{\text{obsd}} = \frac{k_2^{\text{py}}[\text{H}^+][\text{py}] + K_{\text{a}_1}^{\text{py}} k_5^{\text{py}}[\text{py}]}{K_{\text{a}_1}^{\text{py}} + [\text{H}^+]} + (k_{-2}^{\text{py}} + k_{-5}^{\text{py}}[\text{OH}^-]) \quad (9)$$

eq 9 could not be affected. With this in mind we assumed that the k_5^{py} and the k_{-5}^{py} paths were negligible. Equation 9 reduced then to eq 10. The solid line in Figure 8 is the least

$$k_{\text{obsd}} = \frac{k_2^{\text{py}}[\text{py}][\text{H}^+]}{K_{\text{a}_1}^{\text{py}} + [\text{H}^+]} + k_{-2}^{\text{py}} \quad (10)$$

squares fit of the data to eq 10. The value of k_2^{py} was $(3.55 \pm 0.01) \times 10^3$ M^{-1} s^{-1} at 25 °C. This compares favorably with the value of $(3.21 \pm 0.11) \times 10^3$ M^{-1} s^{-1} determined at pH 2. The computer value for k_{-2}^{py} was 0.0121 ± 0.0680 s^{-1} at 25 °C. The value of k_{-2}^{py} determined at pH 2 was 0.0356 ± 0.0055 s^{-1}. Again this is in fair agreement. Because of this good agreement between the parameter at pH 2 and at higher pH, it is concluded that eq 10 adequately describes the data and that the k_5^{py} and k_{-5}^{py} paths are negligible. Since the least-squares fit of this data gave k_{-2}^{py} equal to 0 within one standard deviation, the values of $K_{\text{a}_1}^{\text{py}}$ were calculated by setting $k_{-2}^{\text{py}} = 0$. If k_{-2}^{py} is set equal to 0, then eq 10 can be rearranged to give eq 11.

$$1/k_{\text{obsd}} = \frac{K_{\text{a}_1}^{\text{py}}}{k_2^{\text{py}}[\text{py}][\text{H}^+]} + \frac{1}{k_2^{\text{py}}[\text{py}]} \quad (11)$$

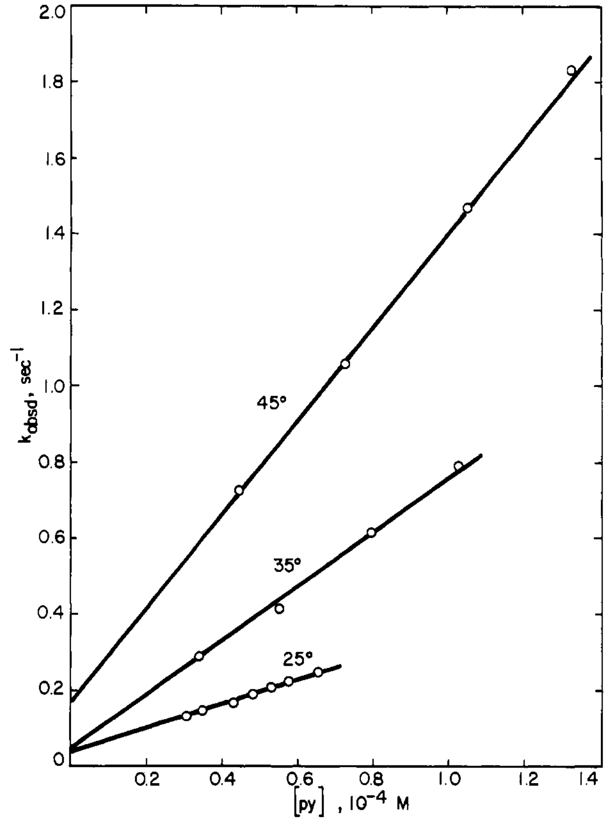

Figure 7. Dependence of k_{obsd} upon [py] for the k_2^{py} path at pH 2.00 and μ = 1.00 M (NaClO_4). The solid lines are the computer fit of the data to eq 5.

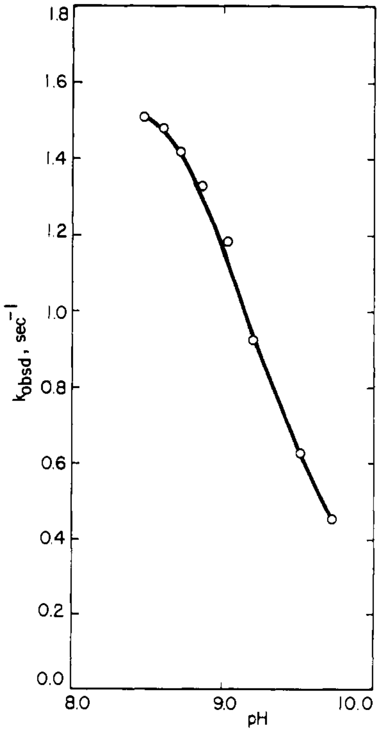

Figure 8. Dependence of k_{obsd} upon pH for the formation of $\text{Co(TPPS)(py)}_2^{3-}$ at 25 °C, [py] = 5.11×10^{-5} M, and μ = 1.00 M (NaClO_4). The solid line is the computer fit of the data to eq 10.

A least-squares fit of $1/k_{\text{obsd}}$ vs. $1/[\text{H}^+]$ would give a straight line with a slope of $K_{\text{a}_1}^{\text{py}}/k_2^{\text{py}}[\text{py}]$. Since k_2^{py} and [py] are known, $K_{\text{a}_1}^{\text{py}}$ can be calculated. These values are reported in Table II.

Scheme II

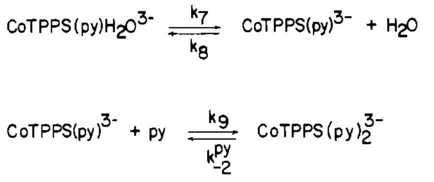

The addition of the second py was studied also at 0.100 M NaOH and high py concentration. Under these conditions, the py dependence became less than linear. The plots of k_{obsd} vs. [py] are shown in Figure 9. The solid lines are the least-squares fit of the data to eq 12. The values of F were

$$k_{obsd} = \frac{E[py] + FG}{G + [py]} \qquad (12)$$

fixed at the values of k_{-2}^{py}. The parameter E is interpreted to be k_7' and G to be k_8/k_9 (Scheme II). The values of k_7 and k_8/k_9 are reported in Table IV. The activation parameters associated with k_7 are reported also in Table IV.

Discussion

Equilibrium Constants. The first acid dissociation constant of Co(TPPS)$(H_2O)_2^{3-}$ is within a factor of 100 of Co(TMpyP)$(H_2O)_2^{5+}$ and Co(TCPP)$(H_2O)_2^{3-}$ at 25 °C with that of (TMpyP)$(H_2O)_2^{3-}$ being slightly larger and that of Co(TCPP)$(H_2O)_2^{3-}$ being smaller.[9,10,15] It has been suggested that these relative values simply imply that the electron density on cobalt increases in the order of Co(TMpyP)$(H_2O)_2^{5+}$, Co(TPPS)$(H_2O)_2^{3-}$, and Co(TCPP)$(H_2O)_2^{3-}$.[9] However, K_{a_1} is 5 times greater for Co(TPPS)(OH)H_2O^{4-} than for Co(TMpyP)(OH)H_2O^{4+}. This is the opposite of the above trend. The values of $K_{a_1}^{py}$ decrease in the order of Co(TMpyP)$(H_2O)py^{5+}$, Co(TPPS)$(H_2O)py^{3-}$, and Co(TCPP)$(H_2O)py^{3-}$,[10] again implying that the electron density in cobalt increases in this order. The values of the py stability constants are reported in Table III. The agreement among the derived and determined constants generally is very good. As the trans ligand changes from H_2O (K_1^{py}) to OH^- (K_4^{py}) to py (K_2^{py}), the value of K_i^{py} changes from 10^8 to 10^5 M^{-1}. The same trends for K_1^L and K_2^L are noted for NCS^- and other cobalt(III) porphyrins (Table V). This decrease in the stability constants is what one would expect if OH^-, NCS^-, and py were placing more electron density on cobalt than on H_2O.

The value of K_1^{py} is greater for Co(TPPS)$(H_2O)_2^{3-}$ than those for Co(TMpyP)$(H_2O)_2^{5+}$ and Co(TCCP)$(H_2O)_2$ which are about the same (Table V). This is surprising since the values of K_1^L for NCS^- and I^- are all similar for the three complexes with those for Co(TMpyP)$(H_2O)_2^{5-}$ being slightly larger, as expected. The values for K_2^{py} for the three complexes (Table V) are all similar, with that of Co(TPPS)$(H_2O)py^{3-}$ being slightly larger. The value of K_4^{py} for Co(TPPS)(OH)H_2O^{4-} is again about 100 times that for Co(TMpyP)(OH)H_2O. These results are inconsistent with the idea that the values of K_i^L should decrease as the ability of the porphyrin to donate electron density to the cobalt(III) increases. Clearly, other factors are important and more data are needed.

Kinetics. The kinetics of the reaction of the addition of the first py will be discussed first. The order of the values of k_1^{py} are Co(TMpyP)$(H_2O)_2^{5+}$ < Co(TPPS)$(H_2O)_2^{3-}$ < Co(TCPP)$(H_2O)_2^{3-}$ (Table V). This is the same ordering as for NCS^- and I^-. This is consistent with the previous suggestion that as the available electron density from the porphyrin that could interact with Co(III) decreases, the rate constant decreases.[9]

Table V. Summary of the Kinetic and Equilibrium Data for Various Cobalt Porphyrins

L	Co(TMpyP)$(H_2O)_2^{5+}$				Co(TPPS)$(H_2O)_2^{3-}$ [c]				Co(TCPP)$(H_2O)_2^{3-}$	
	k_1^L, M^{-1} s^{-1}	K_1^L, M^{-1}	ΔH^*, kcal/mol	ΔS^*, cal/(deg mol)	$10^{-2}k_1^L$, M^{-1} s^{-1}	K_1^L, M^{-1}	ΔH^*, kcal/mol	ΔS^*, cal/(deg mol)	k_1^L, M^{-1} s^{-1}	K_1^L, M^{-1}
py	0.7[a]	10^6 [a]			9.56 ± 0.03	(2.26 ± 0.50) × 10^8	17.6 ± 0.4	14.4 ± 1.3	1.4 × 10^3	⩾10^6
NCS^-	2.92 ± 0.57[b,e]	(6.40 ± 1.55) × 10^3 [b,e]	19.0 ± 2.0[b,e]	7.4 ± 6.8[b,e]	3.24 ± 0.02	(2.64 ± 0.38) × 10^3	18.4 ± 1.1	14.4 ± 3.7	4.50 × 10^2	2.93 × 10^3
I^-	1.62 ± 0.10[b]	(4.00 ± 0.56) × 10^6	20.3 ± 0.5[b]	10.4 ± 1.5[b]	1.18 ± 0.01	(1.14 ± 0.11) × 10	20.8 ± 1.1	20.7 ± 3.6		

L	Co(TMpyP)$(H_2O)_2^{5+}$		Co(TPPS)$(H_2O)_2^{3-}$ [c]				Co(TCPP)$(H_2O)_2^{3-}$	
	k_2^L, M^{-1} s^{-1}	K_2^L, M^{-1}	$10^{-3}k_2^L$ [e], s^{-1}	K_2^L [e], M^{-1}	ΔH^* [e], kcal/mol	ΔS^* [e], cal/(deg mol)	k_2^L, M^{-1} s^{-1}	K_2^L, M^{-1}
py	2.8[a]	4.8 × 10^4 [a]	3.16 ± 0.13	(1.15 ± 0.09) × 10^5	11.6 ± 3.1	−5.1 ± 10.1	2.1 × 10^3	9.5 × 10^4
NCS^-	2.8 × 10^4 [a]	13.7 ± 1.1[b]		2.78 ± 0.84			1.8 × 10^6	6.2
I^-	<1							

L	Co(TMpyP)$(H_2O)_2^{5+}$		Co(TPPS)$(H_2O)_2^{3-}$ [c]				Co(TPP)$(H_2O)_2^{3-}$
	k_4^L, M^{-1} s^{-1}	K_4^L, M^{-1}	k_4^L, M^{-1} s^{-1}	K_4^L, M^{-1}	ΔH^*, kcal/mol	ΔS^*, cal/(deg mol)	k_4^L, M^{-1} s^{-1}
py	2.20 × 10^2	9 × 10^3 [a]	(1.31 ± 0.14) × 10^6	(1.36 ± 0.28) × 10^6	11.5 ± 0.5	6.4 ± 1.6	1.8 × 10^4
NCS	1.10 × 10^2 [a]		1.37 × 10^3	<<1			3.3 × 10^3

[a] Reference 7. [b] Reference 6. [c] References 8 and 9, and this work. [d] Reference 10. [e] Parameters for a D mechanism.

---

(15) TCPP = *meso*-tetrakis(*p*-carboxyphenyl)porphyrin. TMpyP = *meso*-tetrakis(4-*N*-methylpyridyl)porphyrin.

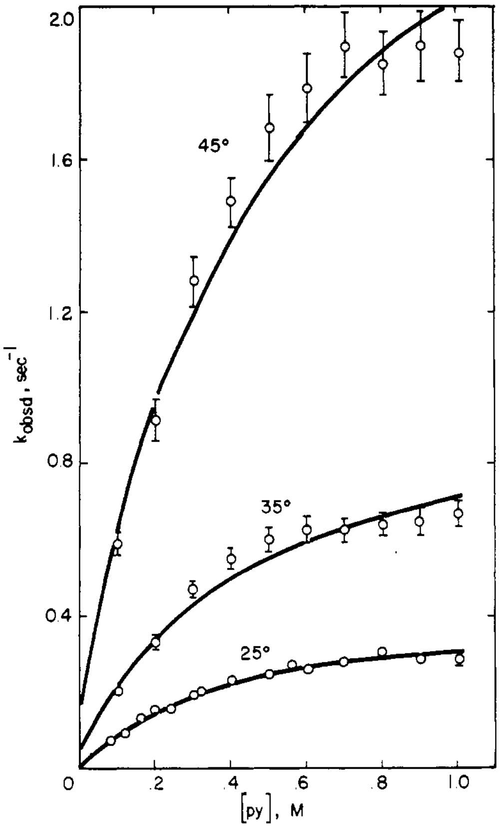

Figure 9. Dependence of k_{obsd} upon [py] for the formation of $Co(TPPS)(py)_2^{3-}$ at μ = 1.00 M ($NaClO_4$) and 0.100 M OH^-. The solid lines are the computer fit of the data to eq 12.

The values of K_1^L for $Co(TPPS)(H_2O)_2^{3-}$ and py, NCS^-, and I^- vary by a factor of 10^7 while the values of k_1^L vary by a factor of 8. This is indicative of dissociative activation. The positive values of ΔS^* also imply dissociative activation. The available activation parameters are reported in Table V. The ΔH^* values are all 19.2 ± 1.6 kcal/mol. This is a remarkably small span for such diverse ligands. Again, this implies dissociative activation. And indeed, the reaction of NCS^- with $Co(TMpyP)(H_2O)_2^{5+}$ occurs via a D mechanism. The values of ΔS^* for the reactions are all positive but range from 7 to 21 cal/(deg mol). Again the same sign and similar values imply dissociative activation.

The value of k_4^{py} was determined under conditions at which $Co(TPPS)(OH)_2^{5-}$ was the predominate species. Within the limit of error of the measurements, the k_6^{py} and k_{-6}^{py} paths were found to be negligible. The replacement of an OH^- ligand by any other ligand generally is not observed in other coordination complexes.

In the base aquation of $Co(NH_3)_5X^{2+}$, where X^- is Cl^-, Br^-, and NO_3^-, it has been shown that H_2O not OH^- is the entering group. By microscopic reversibility this means that for the anation of $Co(NH_3)_5OH^{2+}$ H_2O not OH^- would be the leaving group.[16] Also, in the base aquation of $Co(CN)_5X$, where X = N^{3-}, Br^-, or I^-, H_2O not OH^- is the entering group. Again by microscopic reversibility H_2O not OH^- would be the leaving group in the anation reaction.[17,18] However, in $Co(H_2NC_2H_4NH_2)_2SO_3OH$, OH^- is a leaving group when SO_3^{2-} is the entering group.[19]

The trans labilizing effect of OH^- has been noted in $Co(TMpyP)(H_2O)_2^{5+}$ and $Co(TCPP)(H_2O)_2^{3-}$. The values of k_1^{py}/k_4^{py} for $Co(TMpyP)(H_2O)_2^{5+}$, $Co(TPPS)(H_2O)_2^{3-}$, and $Co(TCPP)(H_2O)_2^{3-}$ are 314, 1.37 × 10^3, and 13, respectively (Table V). Clearly there is no trend as there was with k_1^{py}. The activation parameters associated with k_4^{py} indicate that the increase is primarily due to a decrease in ΔH^* by about 6 kcal. This is consistent with the idea that OH^- places more electron density on cobalt(III) than H_2O does. This then weakens the trans bond. The positive value of ΔS^* implies dissociated activation.

The addition of the second py was studied under three different sets of conditions. Under the first condition (0.01 M H^+), $Co(TPPS)(py)H_2O^{3-}$ was the predominate species. Under the second conditions (pH 8.47–9.72), $Co(TPPS)(py)H_2O^{3-}$ and $Co(TPPS)(py)OH^{4-}$ were both present. $Co(TPPS)(OH)_2^{5-}$ was the predominate species under the third condition (0.100 M NaOH).

In the Results, the conclusion that the k_5^{py} was negligible was reached. This is consistent with the observation that the k_6^{py} path is also negligible, i.e., OH^- is a poor leaving group. This means that the k_2^{py} path is the only one for the formation of $Co(TPPS)(py)_2^{3+}$ at all pH values. Hence the data at 0.01 M H^+ and 0.10 M OH^- should be consistent with each other. Clearly Figure 7 and 9 are not of the same form. Notice that at 0.01 M H^+ the py concentration was about 10^{-4} M whereas at 0.10 M OH^- the py concentration was about 1 M.

Two mechanisms for the k_2^{py} path that result in a k_{obsd} of the form of eq 12 are an S_N1IP and a dissociative (D) one. The SN_1IP mechanism is deemed unlikely in view of py having a zero charge. However, it can not be completely discounted. The D mechanism is illustrated in Scheme II. The rate law for this mechanism would be eq 13. Under pseudo-first-order

$$\frac{d[Co(TPPS)(py)_2^{3-}]}{dt} = \{k_7[py][Co(TPPS)(py)H_2O^{3-}] - k_{-2}^{py}k_8/k_9[Co(TPPS)(py)_2^{3-}]\}/\{k_8/k_9 + [py]\} \quad (13)$$

conditions and the realization that $Co(TPPS)(py)OH^{4-}$ is the predominate species, eq 13 can be integrated to give the pseudo-first-order rate constant (eq 14).

$$k_{obsd} = (k_7'[py] + k_{-2}^{py}k_8/k_9)/(k_8/k_9 + [py]) \quad (14)$$

$$k_7' = k_7/\left[\frac{K_w/[OH^-]}{K_w/[OH^-] + K_{a_1}^{py}}\right]$$

If [py] is less than about 0.02 M and $[OH^-]$ is less than about 10^{-6}, eq 14 becomes $k_{obsd} = ((k_7k_9/k_8)[py]) + k_{-2}^{py}$. This is the form of the equation observed in acid solution with $k_2^{py} = k_7k_9/k_8$. The slope of the tangent of the k_{obsd} vs. [py] plot in 0.100 M OH^- at [py] = 0 should be equal to k_2^{py}. After correction for the presence of $Co(TPPS)(py)OH^{4-}$, the estimated value is (3.3 ± 0.6) × 10^3 M^{-1} s^{-1}. The uncertainty is estimated. This is in good agreement with the value of (3.16 ± 0.13) × 10^3 M^{-1} s^{-1} for k_2^{py} in 0.01 M H^+.

This k_2^{py} path is a very good example if the problem of defining fully a rate law for a reaction. Without the good fortune of being able to study the k_2^{py} path under conditions (high pH) that reduced the concentration of $Co(TPPS)(py)H_2O^{3-}$ and slowed down the reaction rate, an incorrect rate law would have been observed. In this particular case, the values of k_2^{py} and k_7 differ only by a factor of ~2 and the activation parameters associated with k_2^{py} and k_7 are similar.

The value of the activation parameters associated with k_7 are somewhat surprising. Generally when Co(III) reacts via a D or I_d mechanism, the value of ΔH^* is about 20 kcal/mol and the value of ΔS^* is about 10 cal/(deg mol).[6] The lower value of ΔH^*_7 is consistent with the idea that py places more electron density on cobalt(III) than H_2O does. The value of ΔS^*_7 is hard to rationalize. It may reflect the difference in

---

(16) Green, M.; Taube, H. *Inorg. Chem.* **1963**, *2*, 948.
(17) Gould, R. F., Ed. "Mechanisms of Inorganic Reactions"; American Chemical Society: Washington, D.C., 1965; Chapter 2.
(18) Adamson, A. W.; Basolo, F. *Acta Chem. Scand.* **1955**, *64*, 778.
(19) Stranks, D. R.; Yandell, J. K. *Inorg. Chem.* **1970**, *9*, 751.

solvation of Co(TPPS)(py)$^{3-}$. It is interesting to note that the activation parameters associated with k_2^{py} are similar to those of the k_4^{py} path. Clearly $OH^- > py > H_2O$ in labilizing the trans ligand in Co(TPPS)$(H_2O)_2^{3-}$ when py is the entering ligand and H_2O is the leaving group. This same ordering is found in Co(TMpyP)$(H_2O)_2^{5+}$ and Co(TCCP)$(H_2O)_2^{3-}$ (Table V). However the relative differences are not as great as for Co(TPPS)$(H_2O)_2^{3-}$. The combined labilizing effects of the porphyrin and the trans ligand must wait additional information in order to be understood.

Acknowledgment. This research was supported by the Robert A. Welch Foundation, Houston, Texas. J.G.L. wishes to express his gratitude to the Robert A. Welch Foundation and the South African CSIR for financial support as well as the University of the Orange Free State, Bloemfontain, South Africa, for granting the leave.

Registry No. CoTPPS$(H_2O)_2^{3-}$, 58881-09-7; py, 110-86-1; CoTPPS(py)H_2O^{3-}, 77342-06-4; CoTPPS$(py)_2^{3-}$, 77342-07-5; CoTPPS(OH)H_2O^{4-}, 59366-37-9; CoTPPS(OH)py^{4-}, 77342-08-6; CoTPPS$(OH)_2^{5-}$, 77342-09-7; Na_3Co(TPPS)$(H_2O)_2$, 77342-10-0.

Notes

Contribution from the Department of Chemistry,
University of New Hampshire, Durham, New Hampshire 03824

Hydrolysis of Chlorodiphenylphosphine Complexes of Molybdenum and Palladium

Edward H. Wong* and Fontaine C. Bradley

Received November 10, 1980

Coordination of the chlorodiphenylphosphine ligand to transition metals appears to stabilize the P–Cl bond toward hydrolysis, a normally facile process for the free ligand.[1] Under basic conditions, however, Kraihanzel has reported the successful hydrolysis of the cis isomer of bis(chlorodiphenylphosphine)molybdenum tetracarbonyl, $(CO)_4Mo(PPh_2Cl)_2$, to give an anionic product containing a P–O–H–O–P chelate ring (Figure 1).[2]

Austin studied the hydrolysis of *cis*-$Cl_2Pd(PPh_2Cl)_2$ and reported the product to be *cis*-$Cl_2Pd(PPh_2OH)_2$ in which diphenylphosphinous acid, the thermodynamically unstable tautomer of diphenylphosphine oxide, was coordinated to the metal.[3,4]

We were interested in the hydrolytic reactivity of the trans isomer of $(CO)_4Mo(PPh_2Cl)_2$ and the resulting products. We also reinvestigated the hydrolysis of *cis*-$Cl_2Pd(PPh_2Cl)_2$ to confirm the identity of the reported compound. We detail here our findings that demonstrate the recurring formation of the same P–O–H–O–P chelate unit in both hydrolysis reactions.

No straightforward synthesis of the trans isomer of $(CO)_4Mo(PPh_2Cl)_2$ has been available to our knowledge. Kraihanzel has isolated this complex as a minor product in the preparation of $(CO)_5MoPPh_2Cl$.[5] Direct substitution on $Mo(CO)_6$ with a slight excess of phosphine resulted in both cis and trans isomers of $(CO)_4Mo(PPh_2Cl)_2$. Careful recrystallization yielded the less soluble trans isomer in pure form as indicated by IR and ^{31}P NMR data (Table I). The cis isomer can be conveniently prepared from *cis*-$(CO)_4$Mo(piperidine)$_2$, a useful precursor to *cis*-$(CO)_4$Mo(phosphine)$_2$ complexes first prepared by Darensbourg (Scheme I).[6]

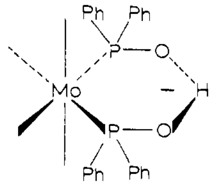

Figure 1.

Table I. ^{31}P NMR Data for the Complexes

complex	chem shift,[a] ppm	solvent
cis-$(CO)_4Mo(PPh_2Cl)_2$	259.7	$CDCl_3$
trans-$(CO)_4Mo(PPh_2Cl)_2$	271.1	$CDCl_3$
cis-$(CO)_4Mo(Ph_2P\text{-}O\text{-}H\text{-}O\text{-}PPh_2)^-$	105.2	$Me_2SO\text{-}d_6$
$[(Ph_2P\text{-}O\text{-}H\text{-}O\text{-}PPh_2)PdCl]_2$	78.1	$CDCl_3$

[a] Referenced to external 85% H_3PO_4; proton decoupled.

Scheme I

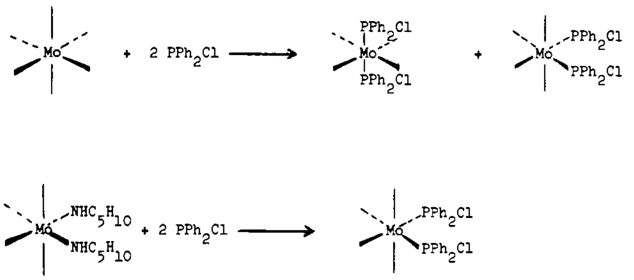

Both *cis*- and *trans*-$(CO)_4Mo(PPh_2Cl)_2$ were found to be stable in neutral or acidic aqueous methanol solutions. We have confirmed Kraihanzel's report that under basic conditions the cis isomer hydrolyzed to give the anionic *cis*-$(CO)_4Mo(Ph_2P\text{-}O\text{-}H\text{-}O\text{-}PPh_2)^-$.[2]

Under identical conditions, the trans isomer gave the same product as supported by IR and ^1H and ^{31}P NMR as well as elemental analyses (eq 1 and 2).

A trans → cis rearrangement has therefore occurred during this reaction. Darensbourg has observed that for normal phosphine ligands, a slight thermodynamic preference for the trans isomer of $(CO)_4$Mo(phosphine)$_2$ exists.[7] This preference is readily overcome here due to the very favorable intramolecular proton bridging available only in the cis product. Many other examples of this P–O–H–O–P chelating unit have been reported. These include complexes of palladium,[8] platinum,[9] and ruthenium[10] in addition to molybdenum.

---

(1) C. S. Kraihanzel, *J. Organomet. Chem.*, **73**, 137 (1974).
(2) G. M. Gray and C. S. Kraihanzel, *J. Organomet. Chem.*, **146**, 23 (1978).
(3) T. E. Austin, Ph.D. Thesis, The University of North Carolina, Chapel Hill, NC, 1966.
(4) L. A. Hamilton and P. S. Landis, "Organic Phosphorus Compounds", Vol. 4, G. M. Kosolapoff and L. Maier, Eds., Wiley, New York, 1972, p 485.
(5) C. S. Kraihanzel and C. M. Bartish, *J. Am. Chem. Soc.*, **94**, 3572 (1972).
(6) D. J. Darensbourg and R. L. Kump, *Inorg. Chem.* **17**, 2680 (1978).
(7) D. J. Darensbourg, *Inorg. Chem.*, **18**, 14 (1979).
(8) A. J. Carty, S. E. Jacobson, R. T. Simpson, and N. J. Taylor, *J. Am. Chem. Soc.*, **97**, 7254 (1975).
(9) R. P. Sperline and D. M. Roundhill, *Inorg. Chem.*, **16**, 2612 (1977).
(10) R. O. Gould, C. L. Jones, W. J. Sime, and T. A. Stephenson, *J. Chem. Soc., Dalton Trans.*, 669 (1977).

0020-1669/81/1320-2333$01.25/0